PCCP

RSC Publishing

PAPER

View Article Online
View Journal | View Issue

Cite this: *Phys. Chem. Chem. Phys.*, 2013, **15**, 1863

Observation of direct vibrational excitation in gas-surface collisions of CO with Au(111): a new model system for surface dynamics

Tim Schäfer,*[ab] Nils Bartels,[ab] Kai Golibrzuch,[ab] Christof Bartels,[ab] Hansjochen Köckert,[ab] Daniel J. Auerbach,[abc] Theofanis N. Kitsopoulos[abd] and Alec M. Wodtke[abc]

Received 24th September 2012,
Accepted 29th November 2012

DOI: 10.1039/c2cp43351f

www.rsc.org/pccp

We report vibrational excitation of CO from its ground (v = 0) to first excited (v = 1) vibrational state in collision with Au(111) at an incidence energy of translation of E_i = 0.45 eV. Unlike past work, we can exclude an excitation mechanism involving temporary adsorption on the surface followed by thermalization and desorption. The angular distributions of the scattered CO molecules are narrow, consistent with direct scattering occurring on a sub-ps time scale. The absolute excitation probabilities are about 3% of those expected from thermal accommodation. The surface temperature dependence of excitation, which was measured between 373 and 973 K, is Arrhenius-like with an activation energy equal to the energy required for vibrational excitation. Our measurements are consistent with a vibrational excitation mechanism involving coupling of thermally excited electron–hole pairs of the solid to CO vibration.

Introduction

A prerequisite to developing a better understanding and predictive theories of surface chemistry is development of a corresponding understanding and theoretical description of the complex sequence of processes often involved in a surface chemical reaction. A key feature that distinguishes surface chemistry from gas-phase chemistry is energy flow between the translational and internal degrees of freedom of a reacting molecule and the elementary excitations of the solid.

Energy transfer to or from the motion of the atoms of the solid lattice (phonons) is an important aspect of this problem.[1–8] For the simple case of dissociation of a diatomic molecule on a surface, building in the effects of lattice motion and the 6 molecular degrees of freedom involves developing a potential energy surface (PES) in 7 or more dimensions and then calculating the dynamical evolution of the system on this PES with the application of classical, quantum, or mixed methods. The challenges here are in many ways similar to gas-phase reactivity in polyatomic molecules; namely, to extend present theories of chemical reactivity to include additional (in this case surface atom) degrees of freedom.

Very different challenges and unanswered questions arise when considering how a solid's electron–hole pair excitations (EHPs) interact with a molecule during a surface collision.[9,10] Electron transfer between the solid and the molecule may take place producing transient negative or positive charge states on the molecule.[11,12] Excited electronic states of the molecule, high in energy in the gas-phase, may be stabilized in the vicinity of the surface. If the solid is a metal, these molecular electronic states may be coupled to the solid's electronic continuum. Local spin conservation at the reaction center may even be destroyed by rapid two electron transfer (as well as $\vec{L}\cdot\vec{S}$ coupling).[13] Another fundamental consideration: one must confront the breakdown of the Born–Oppenheimer (electronically adiabatic) approximation,[14] which forms the basis of nearly all computational chemistry.[15] Hence, heavy atom motion (vibration, translation and rotation) may, in principle, couple with this complex web of electronic interactions.

Understanding electronically nonadiabatic molecular interactions at surfaces is still in its infancy and remains a difficult and important challenge to physical chemistry.[16,17] Obtaining highly detailed and quantitative comparisons between experiment and theory is needed to make progress.[18] State-to-state beam-surface scattering experiments are particularly important

[a] *Institute for Physical Chemistry, Georg-August University of Göttingen, Göttingen, Germany. E-mail: tschaef4@gwdg.de*
[b] *Max Planck Institute for Biophysical Chemistry, Göttingen, Germany. E-mail: alec.wodtke@mpibpc.mpg.de*
[c] *Department of Chemistry and Biochemistry, University of California, Santa Barbara, USA*
[d] *Department of Chemistry, University of Crete and IESL-FORTH, Heraklion, Greece*

in this context as are state-specific studies of reactive desorption, which can be related to scattering data *via* the principle of detailed balance.[19–21] In such experiments a diversity of dynamical properties of scattered molecules, *e.g.* quantum-state,[12] speed[22,23] and angular distributions,[24] can be studied as a function of a wide range of incidence conditions such as: incidence translational,[25] electronic,[26,27] vibrational,[28] and rotational energy[29] at selected incidence angles and surface temperatures. Such data demand high physical accuracy from new theories and test their assumptions in a highly rigorous way.

Testing electronically nonadiabatic theories of molecule–surface interactions at such a rigorous level has, so far, only been possible for a single example, NO interacting with Au(111).[10] Comprehensive benchmark data were able to discriminate between two competing theories of electronically nonadiabatic behavior;[30] Independent Electron Surface Hopping (IESH)[31–33] agreed well with benchmark beam-surface scattering data on vibrational excitation probabilities of NO scattering from Au(111), whereas molecular dynamics with electronic friction failed.[30]

While agreement between experiment and IESH is good for this system, remaining deviations do exist. IESH suffers weaknesses in its ability to predict the NO vibrational excitation probability dependence on incidence energy of translation[30] as well as associated scattering angular and rotational distributions.[34] Very recently, we have found that the translational inelasticity of collisions of NO with Au(111) is poorly reproduced by IESH.[35] Since IESH theory treats only one (a transient anion) excited electronic state of the NO in the surface collision, one may logically ask if some of the remaining deviations from experiment are the result of ignoring the open shell electronic structure of NO. Clearly, a comparison of IESH to an analogous closed electronic shell scattering system would be helpful in addressing this question.

Carrying out state-to-state beam-surface scattering studies for CO colliding with Au(111) offers an ideal direction for researching these issues. It is reasonable to expect that nonadiabatic effects might play a role in vibrational excitation of this system since lifetimes of CO (v = 1) adsorbed on Cu(100) reveal important contributions from electronically nonadiabatic effects.[36–39] Unfortunately, state-to-state scattering experiments have, thus far, been unable to report unambiguous evidence for direct vibrational excitation of CO on any metal.[8] Since this early work, much progress has been made to improve state-to-state scattering experiments.[40] We thought it would therefore be worthwhile to revisit this challenging system.

In this paper we report data on state-to-state scattering of CO from Au(111). We unambiguously observe direct vibrational excitation of CO to its first excited vibrational state. Trapping/desorption can be unambiguously excluded as accounting for the observed vibrational excitation. The surface temperature, T_S, dependence is Arrhenius-like as expected for an electronically nonadiabatic mechanism for direct vibrational excitation.[41,42] These observations open the door to a comprehensive study of many aspects of CO interactions with noble metals, which could serve as an important benchmark for theories of nonadiabatic molecule surface interactions.

Experimental methods

The experiments are carried out in two different apparatus described in detail in previous publications.[40,43] The T_S-dependence of the absolute vibrational excitation probabilities, CO (v = 0 → 1), resulting from CO collisions with an Au(111) surface are obtained using an apparatus described in ref. 43. Briefly, a supersonic molecular beam is produced by expanding 12% CO in H_2 through a piezoelectric actuated nozzle with 3 ATM stagnation pressure at 300 K. The resulting molecular beam produces CO with E_I = 0.45 eV and a FWHM for the energy distribution of 0.06 eV. The skimmed molecular beam (2 mm diameter skimmer, Model 2, Beam Dynamics Inc.) travels through one differential chamber before entering the UHV chamber (base pressure 2×10^{-10} Torr) where it collides with a Au(111) crystal at near normal incidence ($\theta_i < 2^\circ$, where θ_i is the angle of incidence with respect to the surface normal). T_S is varied between 370 and 970 K by resistive heating. The surface of the crystal is cleaned by sputtering with 3 keV Ar^+ and annealing at 1000 K for 20 min. Surface cleanliness is checked by means of Auger electron spectroscopy as in previous work.[44] The populations of CO (v = 0) and CO (v = 1) are measured by 2 + 1 REMPI *via* the $B^1\Sigma^+$ state scanning the Q-branch of the (0,0) and (1,1) bands, respectively. The required light of 230 nm (3 mJ per pulse) is obtained from a frequency doubled Nd:YAG laser (LabPRO 270, Spectra Physics), pumped dye laser (Sirah, PRSC-DA-24). The laser beam is focused using a Suprasil lens (f = 500 mm) and ionizes the scattered molecules at a scattering angle of 20° (with respect to the surface normal) without saturating the two-photon transition.[45]

Scattering angular distributions are measured on an apparatus described in detail in ref. 40, which resembles the experimental setup just described. This apparatus has an additional differentially pumped chamber between the source and the UHV chamber and is equipped with an optical arrangement that makes it possible for us to translate the REMPI beam along a line perpendicular to the molecular beam enabling measurements of scattering angular distributions. The angular divergence of the incoming molecular beam was calculated from the geometry of the instrument to be 1.2°.

Results

REMPI spectra in the vicinity of the $B^1\Sigma^+$ (v = 1) ← $X^1\Sigma^+$ (v = 1) Q-branch band-head are shown as an inset in Fig. 1. Spectra at four values of T_S between 373 and 873 K are shown. A fragment of the O-branch of the (0,0) band and the complete Q-branch of the (1,1) band are clearly seen. Due to nearly equal rotational constants of the $B^1\Sigma^+$ and $X^1\Sigma^+$ states, the Q-branch is highly congested and individual rotational transitions are not resolved. The rotational Q-branch contour in all four REMPI spectra can be fitted assuming a rotational temperature that is independent of T_S.

The integrated intensity of the Q-branch of the (1,1) band increases by about 100 fold as T_S increases from 373 K to 973 K, while the intensity of the lines of the O-branch of the (0,0) band varies by less than a factor of two. This is qualitative evidence of

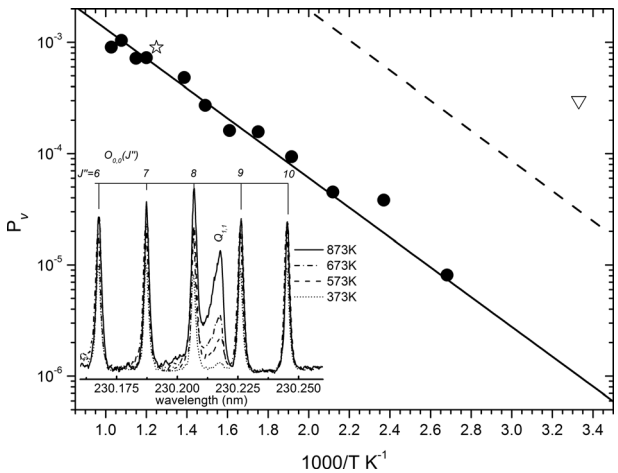

Fig. 1 Vibrational excitation probabilities *versus* inverse surface temperature for an incidence energy of translation of 0.45 eV. Experimentally derived excitation probabilities are shown as closed circles. The solid line results from an Arrhenius fit with $P_v(T_S) = A \exp(-\Delta E_{vib}/k_B T_S)$. Here, P_v is the absolute vibrational excitation probability, ΔE_{vib} is the vibrational excitation energy of 2143 cm^{-1}, k_B is the Boltzmann constant and A(= 0.021) is the pre-factor, which within the context of an electronically nonadiabatic mechanism describes the absolute coupling strength of EHP and molecular vibration.[1] The dashed line denotes the thermal limit. The inset shows the REMPI spectra of surface scattered CO using the $B^1\Sigma^+ \leftarrow X^1\Sigma^+$ transition for temperatures of 373 K, 573 K, 673 K and 873 K (bottom to top). As T_S increases, the Q-branch of the (1,1) band increases about 100 fold, whereas the O-branch of the (0,0) band increases by less than a factor of 2. The star, referred to us lovingly as ''Checkpoint Charlie'', denotes the excitation probability measured in ref. 8 for an incidence kinetic energy of 0.7 eV. The downward pointing triangle was also reported as an upper limit to the vibrational excitation probability.

the strong T_S-dependence of the population observed in CO (v = 1), clearly showing that the vibrational excitation of CO is strongly coupled with the thermal energy of the solid. The ratio of the integrated Q-branch intensities of the (1,1) and (0,0) bands is used to calculate the absolute vibrational excitation probability – CO (v = 0 → 1) due to collision with Au(111) – in a quantitative fashion analogous to previous work on NO scattering from Au(111).[44,46] Great care was taken to correct for vibrationally elastic scattering of thermally populated CO (v = 1) in the incident beam. The narrow Q-branch of the (0,0) band is blue shifted by 0.17 nm with respect to the likewise narrow Q-branch of the (1,1) band; hence, the two bands are spectrally well separated as shown in Fig. 3 of ref. 8. Since the two bands are narrow and near to one another, scanning the laser back and forth between and across these two bands is a simple matter performed in a short time. By using the integrated Q-branch intensity ratio between the (0,0) and the (1,1) bands, no Hönl–London factors need to be taken into account to obtain the vibrational excitation probability. Since the laser pulse energy used here does not saturate the $B^1\Sigma^+ \leftarrow X^1\Sigma^+$ transition, the computed numbers are normalized to the measured laser power dependence[47,48] and Franck–Condon factors of the $B^1\Sigma^+ \leftarrow X^1\Sigma^+$ system.[49] The observed power dependence shows that only the ionization step in the 2 + 1 REMPI is saturated. For each vibrational state, the voltage across the MCP was adjusted to avoid saturation and the relative signal was calculated using the measured gain curve of the MCP.

Excitation probabilities derived in this way are displayed in Fig. 1 (as solid circles) for 373 K ≤ T_S ≤ 973 K in an Arrhenius plot assuming no significant angular dependence of the vibrational excitation. The solid line in Fig. 1 is a fit to the derived excitation probabilities, P_v, of the form: $P_v(T_S) = A \exp(-\Delta E_{vib}/kT_S)$, where the effective activation energy, ΔE_{vib}, is the vibrational excitation energy to populate CO (v = 1) from CO (v = 0). The dashed line shows the vibrational excitation probability that would result if CO vibration came to full thermal equilibrium with the solid. Observed excitation probabilities are uniformly 3% of this so-called thermal limit.[1] Also displayed in Fig. 1 (as a star) is the excitation probability for E_I = 0.7 eV and T_S = 800 K reported in ref. 8. The downward pointing open triangle is an upper limit to the vibrational excitation probability for E_I = 0.7 eV and T_S = 300 K also reported in ref. 8.

Scattering angular distributions for the channels CO (v = 0 → 0) and CO (v = 0 → 1) are shown in Fig. 2 at three values of T_S (= 573, 773 and 973 K). The scattering angular distributions are very similar for the two vibrational channels and clearly show no angular dependence on the vibrational excitation. In all cases the angular distributions are narrow (between $\cos^5\theta$ and $\cos^9\theta$) and peak near the specular scattering angle. Careful inspection reveals that the scattering angular distributions all become slightly broader with increasing T_S. Also shown in Fig. 2 (as dotted lines) are $\cos\theta$ functions, which are substantially broader than the observed scattering angular distributions.

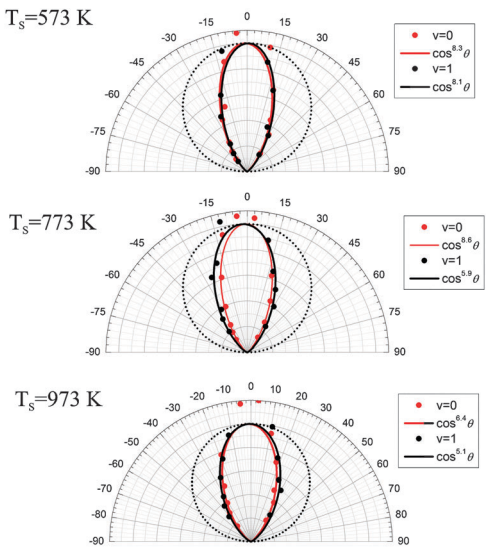

Fig. 2 Angular distributions of CO (v = 0 → 0) (red circles) and CO (v = 0 → 1) (black circles) for E_I = 0.45 eV. The laser wavelength was set near the peak of the (1,1) Q-branch and the O (1,0) branch of the (0,0) band. Therefore it reflects the behavior of several low rotational states for CO (v = 1) while representing only J = 10 for CO (v = 0). Solid lines are best fits to the data. Also shown in each plane is a $\cos\theta$ angular distribution as a dotted line, expected for trapping/desorption, where the trapping probability is independent of incidence angle. Note a slight broadening of all angular distributions with increasing T_S as expected for a direct scattering mechanism. The data points near 0° are subject to background due to non-resonant ionization of the incident beam.

Discussion

An extensive study has been previously published employing an experimental setup similar to the present work.[8] In that work, continuous supersonic beams of CO were formed by seeding in H_2 or He and employing variable nozzle temperature, T_{Nozzle}, to influence the incidence energy of translation. When these CO beams were scattered from a Au(111) crystal, CO ($v = 0$ and 1) were observed by 2 + 1 REMPI *via* the $B^1\Sigma^+ \leftarrow X^1\Sigma^+$ system, similar to this work. In one measurement at $E_I = 0.7$ eV and $T_S = 300$ K ($T_{Nozzle} = 300$ K) no CO ($v = 1$) could be observed, hence, only an upper limit to the excitation probability, $P_v < 3 \times 10^{-4}$, could be reported. This is shown as a downward pointing triangle in Fig. 1. In another experiment, $E_I = 0.7$ eV and $T_S = 800$ K ($T_{Nozzle} = 300$ K), shown as a star in Fig. 1, a signal from CO ($v = 1$) could be seen clearly. Attempts to induce higher vibrational excitation probabilities by heating the nozzle and thereby increasing E_I were compromised by the increased population of incident CO ($v = 1$) in the molecular beam, which is a source of unwanted background due to vibrationally elastic rotational redistribution occurring in collision with the surface.

Compared to the present work, which benefits from many experimental improvements, most importantly the use of pulsed molecular beams and the very short distance between the nozzle and surface, it seems that the 1993 work was fundamentally less sensitive to scattering channels exhibiting small absolute excitation probabilities. Scattering probabilities below 3×10^{-4} were not reported in ref. 8; while in the present work, we observe values as small as $P_v = 8 \times 10^{-6}$ (*e.g.* at $E_I = 0.45$ eV and $T_S = 373$ K). Presumably due to the lack of the required sensitivity to small signals, additional measurements of angular distributions and other potential dynamical indicators could not be undertaken. In the absence of a more comprehensive data-set, it was impossible to observe dynamical fingerprints of a direct scattering mechanism that had produced the CO ($v = 1$) observed in that work. Hence, it was thought more likely that trapping/desorption produced the observed CO ($v = 1$), a process that is simply the result of the molecule reaching thermal equilibrium with the solid due to its long interaction time. This possibility was supported by measurements of trapping probability (using the King and Wells method) which were found to scale as $E_I \cos\theta_I$, where θ_I is the incidence angle. In addition, CO ($v = 1$) survival probabilities were measured using a heated nozzle. No CO ($v = 1$) loss could be seen although CO ($v = 1$) survival probabilities as low as 0.9, 0.9 and 0.6 would not have been distinguished from complete survival for $E_I = 0.23$, 0.63 and 1.1 eV, respectively.

These narrow scattering angular distributions are unambiguous proof that trapping/desorption does not substantially contribute to the signals observed in this work. Fig. 2 shows (as dotted lines) a $\cos\theta_i$ angular distribution which is the distribution that would be expected if the trapping probability were independent of θ_i. As mentioned above, CO trapping on Au(111) was found to scale with $E_I \cos\theta_I$.[8] Similar observations have been made for Ar trapping on hydrogen-terminated tungsten, 2H-W(100). In that work thermal desorption was also studied and angular distributions broader than $\cos\theta_i$ were observed and rationalized on the basis of detailed balance.[50]

A finer point concerning the scattering angular distributions is the slight broadening with increasing T_S, which we interpret as the influence of thermal Au atom motion increasing the potential energy surface's corrugation.[30] This is to be compared with the dramatic broadening of thermal desorption angular distributions observed with increasing T_S for Ar desorbing from 2H-W(100). See Fig. 7–9 in ref. 50.

Further evidence that the observed CO ($v = 1$) does not originate from a trapping/desorption mechanism is found in the rotational state distributions of these molecules. If the signals observed here were due to trapping/desorption, the observed rotational distributions of CO ($v = 1$) would depend on T_S, which they do not.

While additional experimental and theoretical work is needed, we point out that the T_S dependence of the vibrational excitation probabilities is consistent with an electronically nonadiabatic vibrational excitation mechanism. As has been pointed out repeatedly, the population of hot electron–hole pairs with energy sufficient to excite a vibrational transition with energy ΔE_{vib} is accurately described by an Arrhenius-like relation, $A \exp(-\Delta E_{vib}/kT_S)$, over a wide range of T_S. Hence the slope of the solid line in Fig. 1, which is found to be $\Delta E_{vib}/k$, suggests that the vibrational excitation probability is limited by the population of hot EHPs of appropriate energy. The pre-exponential factor obtained from this fit, $A = 0.021$, is about 13× smaller than that obtained for a similar analysis of NO in collision with Au(111),[46] suggesting that the strength of the electronically nonadiabatic coupling is substantially lower for CO/Au(111) than for NO/Au(111).[1] This might reflect the different electron affinities for NO and CO, 0.15 eV and −1.5 eV, respectively, and how these energetics modify electron transfer dynamics between the molecule and the solid.[10] This energetic difference implies that the image charge stabilization of the CO anion results in an anion crossing with the neutral CO potential surface at a relatively high total energy in comparison to the analogous NO crossing. Hence, for a given $E_I = 0.45$ eV, the formation of a transient negative ion state might be less likely for the CO/Au system than for the NO/Au system. See also ref. 18.

Conclusion

Angular distributions and surface temperature dependent vibrational excitation probabilities for collisions of CO on a Au(111) surface have been experimentally derived. The outcomes of both experiments strongly support the picture of a direct vibrational excitation mechanism, where trapping/desorption plays at most a minor role. The observations presented here are consistent with an electronically nonadiabatic coupling of CO vibration to electron–hole pairs of the Au surface that is about one order of magnitude weaker than for the well-studied NO/Au(111) system.

Acknowledgements

CB, DJA, TK and AMW acknowledge support from the Alexander von Humboldt foundation. We are grateful to Russell Cooper for valuable discussions.

Notes and references

1 D. Matsiev, Z. S. Li, R. Cooper, I. Rahinov, C. Bartels, D. J. Auerbach and A. M. Wodtke, *Phys. Chem. Chem. Phys.*, 2011, **13**, 8153–8162.
2 J. A. Barker and D. J. Auerbach, *Surf. Sci. Rep.*, 1984, **4**, 1–99.
3 A. C. Luntz and J. Harris, *Surf. Sci.*, 1991, **258**, 397–426.
4 C. T. Rettner, D. J. Auerbach, J. C. Tully and A. W. Kleyn, *J. Phys. Chem.*, 1996, **100**, 13021–13033.
5 J. C. Tully, *Annu. Rev. Phys. Chem.*, 2000, **51**, 153–178.
6 S. Nave and B. Jackson, *J. Chem. Phys.*, 2007, **127**, 224702.
7 F. Nattino, C. Diaz, B. Jackson and G. J. Kroes, *Phys. Rev. Lett.*, 2012, **108**, 236104.
8 C. T. Rettner, *J. Chem. Phys.*, 1993, **99**, 5481–5489.
9 A. M. Wodtke, J. C. Tully and D. J. Auerbach, *Int. Rev. Phys. Chem.*, 2004, **23**, 513–539.
10 A. M. Wodtke, D. Matsiev and D. J. Auerbach, *Prog. Surf. Sci.*, 2008, **83**, 167–214.
11 J. W. Gadzuk, *J. Chem. Phys.*, 1983, **79**, 6341–6348.
12 Y. H. Huang, C. T. Rettner, D. J. Auerbach and A. M. Wodtke, *Science*, 2000, **290**, 111–114.
13 C. Carbogno, J. Behler, A. Gross and K. Reuter, *Phys. Rev. Lett.*, 2008, **101**, 096104.
14 M. Born and R. Oppenheimer, *Ann. Phys.*, 1927, **84**, 0457–0484.
15 J. C. Tully, *Theor. Chem. Acc.*, 2000, **103**, 173–176.
16 C. Bartels, R. Cooper, D. J. Auerbach and A. M. Wodtke, *Chem. Sci.*, 2011, **2**, 1647–1655.
17 E. Hasselbrink, *Curr. Opin. Solid State Mater. Sci.*, 2006, **10**, 192–204.
18 I. Rahinov, R. Cooper, D. Matsiev, C. Bartels, D. J. Auerbach and A. M. Wodtke, *Phys. Chem. Chem. Phys.*, 2011, **13**, 12680–12692.
19 U. Leuthausser, *Z. Phys. B: Condens. Matter*, 1983, **50**, 65–69.
20 G. Comsa and R. David, *Surf. Sci. Rep.*, 1985, **5**, 145–198.
21 H. A. Michelsen and D. J. Auerbach, *J. Chem. Phys.*, 1991, **94**, 7502–7520.
22 R. Cooper, I. Rahinov, C. Yuan, X. M. Yang, D. J. Auerbach and A. M. Wodtke, *J. Vac. Sci. Technol., A*, 2009, **27**, 907–912.
23 I. Rahinov, R. Cooper, C. Yuan, X. M. Yang, D. J. Auerbach and A. M. Wodtke, *J. Chem. Phys.*, 2008, **129**, 214708.
24 Q. Ran, D. Matsiev, D. J. Auerbach and A. M. Wodtke, *Nucl. Instrum. Methods Phys. Res., Sect. B*, 2007, **258**, 1–6.
25 C. T. Rettner, D. J. Auerbach and H. A. Michelsen, *Phys. Rev. Lett.*, 1992, **68**, 1164–1167.
26 R. T. Jongma, G. Berden, D. van der Zande, T. Rasing, H. Zacharias and G. Meijer, *Phys. Rev. Lett.*, 1997, **78**, 1375–1378.
27 R. T. Jongma, G. Berden, T. Rasing, H. Zacharias and G. Meijer, *J. Chem. Phys.*, 1997, **107**, 252–261.
28 C. T. Rettner, H. A. Michelsen and D. J. Auerbach, *J. Chem. Phys.*, 1995, **102**, 4625–4641.
29 H. A. Michelsen, C. T. Rettner, D. J. Auerbach and R. N. Zare, *J. Chem. Phys.*, 1993, **98**, 8294–8307.
30 R. Cooper, C. Bartels, A. Kandratsenka, I. Rahinov, N. Shenvi, K. Golibrzuch, Z. Li, D. J. Auerbach, J. C. Tully and A. M. Wodtke, *Angew. Chem.*, 2012, **124**, 5038–5042.
31 S. Roy, N. A. Shenvi and J. C. Tully, *J. Chem. Phys.*, 2009, **130**, 174716.
32 N. Shenvi, S. Roy and J. C. Tully, *Science*, 2009, **326**, 829–832.
33 N. Shenvi, S. Roy and J. C. Tully, *J. Chem. Phys.*, 2009, **130**, 174107.
34 R. Cooper, Z. Li, K. Golibrzuch, C. Bartels, I. Rahinov, D. J. Auerbach and A. M. Wodtke, *J. Chem. Phys.*, 2012, **137**, 064705–064712.
35 To be published.
36 M. Morin, N. J. Levinos and A. L. Harris, *J. Chem. Phys.*, 1992, **96**, 3950–3956.
37 M. Head-Gordon and J. C. Tully, *J. Chem. Phys.*, 1992, **96**, 3939–3949.
38 V. Krishna and J. C. Tully, *J. Chem. Phys.*, 2006, **125**, 054706.
39 M. Headgordon and J. C. Tully, *J. Chem. Phys.*, 1995, **103**, 10137–10145.
40 Q. Ran, D. Matsiev, A. M. Wodtke and D. J. Auerbach, *Rev. Sci. Instrum.*, 2007, **78**, 104104.
41 C. T. Rettner, F. Fabre, J. Kimman and D. J. Auerbach, *Phys. Rev. Lett.*, 1985, **55**, 1904–1907.
42 D. M. Newns, *Surf. Sci.*, 1986, **171**, 600–614.
43 T. Schäfer, N. Bartels, N. Hocke, X. Yang and A. M. Wodtke, *Chem. Phys. Lett.*, 2012, **535**, 1.
44 R. Cooper, I. Rahinov, Z. Li, D. Matsiev, D. J. Auerbach and A. M. Wodtke, *Chem. Sci.*, 2010, **1**, 55–61.
45 Evidence for this is an observed quadratic laser power dependence of the REMPI signal.
46 R. Cooper, Z. S. Li, K. Golibrzuch, C. Bartels, I. Rahinov, D. J. Auerbach and A. M. Wodtke, *J. Chem. Phys.*, 2012, **137**, 064705.
47 We found a dependence of the signal S to laser pulse energy ILaser of $S \propto$ ILaser 1.9.
48 S. Wurm, P. Feulner and D. Menzel, *J. Chem. Phys.*, 1996, **105**, 6673–6687.
49 R. E. Imhof, F. H. Read and S. T. Beckett, *J. Phys. B: At. Mol. Phys.*, 1972, **5**, 896.
50 C. T. Rettner, E. K. Schweizer and C. B. Mullins, *J. Chem. Phys.*, 1989, **90**, 3800–3813.